Structure and Substrate Recognition of the *Staphylococcus aureus* Protein Tyrosine Phosphatase PtpA

Carolina Vega[1], **Seemay Chou**[2], **Katherine Engel**[2], **Maria E. Harrell**[3], **Lakshmi Rajagopal**[3,4], and **Christoph Grundner**[1,5,*]

[1]Seattle Biomedical Research Institute, Seattle, WA

[2]Department of Molecular and Cell Biology, University of California Berkeley, Berkeley, CA

[3]Seattle Children's Hospital Research Institute, Seattle, WA

[4]Department of Pediatric Infectious Diseases, University of Washington, Seattle, WA

[5]Department of Global Health, University of Washington, Seattle, WA

Abstract

Phosphosignaling through pSer/pThr/pTyr is emerging as a common signaling mechanism in prokaryotes. The human pathogen *Staphylococcus aureus* (*S. aureus*) produces two low-molecular weight protein tyrosine phosphatases, PtpA and PtpB, with unknown functions. To provide the structural context for understanding PtpA function and substrate recognition, establish PtpA's structural relations within the protein tyrosine phosphatase family, and to provide a framework for the design of specific inhibitors, we solved the crystal structure of PtpA at 1 Å resolution. While PtpA adopts the common, conserved PTP fold and shows close overall similarity to eukaryotic PTPs, several features in the active site and surface organization are unique and can be explored to design selective inhibitors. A peptide bound in the active site mimics a phosphotyrosine substrate, affords insight into substrate recognition, and provides a testable substrate prediction. Genetic deletion of *ptpA* or *ptpB* does not affect in *vitro* growth or cell wall integrity, raising the possibility that PtpA and PtpB have specialized functions during infection.

Keywords

Protein Tyrosine Phosphatase; crystal structure; *S. aureus*; phosphosignaling; substrate

---

Infections with methicillin resistant *S. aureus* pose a growing public health problem, causing severe mortality and morbidity [1]. Treatment options for methicillin resistant *S. aureus* are highly limited, and resistance to almost all antibiotics has been reported, highlighting the need for new drugs with novel mechanisms of action[2]. Given the success of drugs against human phosphosignaling enzymes [3; 4], their prokaryotic counterparts could provide similarly tractable targets. Histidine kinases of the two component systems were long considered the cornerstone of bacterial phosphosignaling. However, microbial genome sequencing increasingly suggests that "eukaryotic like" pSer/pThr/pTyr kinases and

---

Publisher's Disclaimer: This is a PDF file of an unedited manuscript that has been accepted for publication. As a service to our customers we are providing this early version of the manuscript. The manuscript will undergo copyediting, typesetting, and review of the resulting proof before it is published in its final citable form. Please note that during the production process errors may be discovered which could affect the content, and all legal disclaimers that apply to the journal pertain.

phosphatases are also common and sometimes even more frequent in prokaryotes than two component systems [5; 6].

S. aureus produces two protein tyrosine phosphatases (PTPs), PtpA and PtpB [7]. Sequence similarity groups PtpA and PtpB with the family of low molecular weight protein tyrosine phosphatases (LMW-PTP) or acid phosphatases. The LMW-PTPs share key characteristics of the active site fold with members of the classical tyrosine and dual specificity phosphatase families [8]. However, their topology is largely different. Most notably, the active site P-loop is located in the N-terminal part of the protein, while classical PTPs and dual specificity phosphatases harbor this loop towards the middle of the sequence. These differences suggest that the LMW-PTPs evolved separately from the classical tyrosine and dual specificity phosphatases.

No substrates have been identified for the *S. aureus* PTPs, and only three tyrosine-phosphorylated proteins have been identified in *S. aureus* to date [9; 10], emphasizing our poor understanding of tyrosine phosphorylation in this pathogen. Phosphoproteomic studies in *B. subtilis* and *E. coli* showed that tyrosine phosphorylation relative to Ser/Thr phosphorylation is more common in bacteria than in eukaryotes [11; 12], suggesting that bacteria rely on tyrosine phosphorylation more extensively for cell signaling. To better understand phosphotyrosine signaling in *S. aureus* and to provide the structural underpinnings to explore PtpA as a potential therapeutic target, we solved the PtpA crystal structure at 1 Å resolution. Overall, the structure highlights the conservation of the LMW-PTP fold across kingdoms, defines the structural relation of PtpA within the PTP family, and reveals distinct features in the active site that can be exploited for inhibitor design. A peptide bound in the active site mimics a phosphotyrosine substrate and allows testable predictions of physiologic substrates. Neither PtpA nor PtpB are essential for *in vitro* growth and may play a specialized role during infection.

The LMW-PTP fold is conserved in *S. aureus* PtpA

The PtpA sequence from strain Mu50 was synthesized and cloned into the pHGWA expression vector [13], grown to an OD_{600} of 0.8 in terrific broth, induced with 100 μM Isopropyl β-D-1-thiogalactopyranoside, and expressed over night at 18°C. The PtpA protein was purified by metal affinity chromatography. After cleaving the His6 tag with trypsin (1:1000 w/w) for 15 min at room temperature, the protein was further purified by size exclusion chromatography in 20 mM Tris pH7.5, 100 mM NaCl. Crystals were grown by sitting drop vapor diffusion. PtpA protein (15 mg/ml) was mixed 1:1 with 0.9 M NaH_2PO_4/1.1 M K_2HPO_4 acetate buffer (pH 4.5). The crystal was mounted on a cryoloop and flash-cooled at 100K in crystallization buffer with 20% glycerol as cryoprotectant. Diffraction data were collected at the Lawrence Berkeley National Laboratory Advanced Light Source Beamline 8.3.1. Data were collected to 1 Å resolution at 100K by using 1.11587 Å X-rays and reduced with the HKL2000 program suite [14]. PtpA crystallized in space group P1211 with one molecule in the asymmetric unit. The structure was solved by molecular replacement using MolRep [15] and Protein Data Bank-ID 2CWD as the search model. ARP/wARP [16] was used to rebuild the structure. Building and refinement were performed using cycles of model building with Coot [17] and refinement with Phenix [18]. After modeling the PtpA protein chain, waters and heteroatoms were built. Large continuous electron density covering the active site cavity remained after building the entire PtpA protein chain and heteroatoms. This density clearly defined seven well-ordered amino acid residues including five histidine residues originating from the cleaved His6 tag used for protein purification. The structure was refined with riding hydrogens, anisotropic individual *B*-factors (except for hydrogens and solvent) and optimization of stereochemical and X-ray restraints in Phenix [18]. The final PtpA crystal structure comprises 153 of the 154 PtpA

residues, a five-residue vector sequence at the N-terminus, the seven amino acid long peptide, 297 water molecules, and two phosphates. The structure was refined to an R_{work} of 15% and an R_{free} of 16.8% (Table 1). The R_{free} was calculated by using a random 5% of the data. The structure was deposited to the Protein Data Bank under ID code 3ROF.

The PtpA fold and topology follows the general architecture of LMW-PTPs (Figure 1A). PtpA adopts a single domain, α/β fold with a central four-stranded parallel β-sheet providing the scaffold for the active site. The catalytic cysteine, Cys8, is positioned in the P-loop connecting sheet 1 and helix 1. Well defined tetrahedral electron density cradled by the P-loop identified a phosphate (Figure 1B), which is commonly found in structures of PTPs. The P-loop comprises residues 8 to 15 and is defined by the signature CX_4CR motif common to LMW-PTPs. Five helices are arranged around this core motif. One side of PtpA is defined by helix 5, a long helix with a kink introduced by a 3_{10} helical segment. The opposite side of the molecule is composed of two 12 and 18 amino acid long loop regions that wrap around PtpA. These loops are well ordered and each stabilized by three β-turns. A second cysteine, Cys13, is present in the P-loop. This cysteine is highly conserved in LMW-PTPs and is thought to confer protection of the catalytic cysteine from oxidative inactivation through the formation of a reversible intramolecular disulfide bond [19]. The active site cavity is defined by two loop regions. The loop connecting sheet 2 and helix 2 shapes the outer limits of one side of the cavity. Opposite this region, the loop between sheet 4 and helix 5 delineates the other side of the active site cavity. Based on the structural overlay of PtpA with human LMW-PTP, we identified Asp120 as the general acid. Site directed mutagenesis of Asp120 to Ala abrogates activity of PtpA with the artificial phosphatase substrate para-nitrophenol phosphate, confirming its essentiality for function, likely by serving as the general acid (data not shown). Two adjacent tyrosine residues, Tyr122 and Tyr123, contribute to the deepening of the active site pocket to >8 Å, likely excluding pSer and pThr as potential substrates.

PtpA has unique features

PtpA and PtpB share sequence similarity of 50% and identity of 27%. Surprisingly, the similarity of *S. aureus* PtpA to the human LMW-PTP is higher than that to PtpB, with 52% similarity and 35% identity. The closest bacterial sequence homolog is an LMW-PTP from *Geobacillus thermodenitrificans* with 72% and 50% similarity and identity, respectively. The closest structural homologue of PtpA by Z-score in the Protein Data Bank identified by the DALI server [20] is the B-form of human LMW-PTP, HPTP-B. The Cα root mean square deviation (rmsd) between PtpA and HPTP-B [21] is 1.6 Å over 749 atoms, highlighting the close similarity between the human and bacterial PTPs, with only few differences in the general fold (Figure 2A). The closest microbial homologue in the Protein Data Bank is a LMW-PTP from *Thermos thermophilus* (2CWD), with a Cα rmsd of 1.7 Å. Main differences to other PTP structures are found mainly in three loop regions. Two of these loops are on the periphery of the molecule, while loop 2 is close to the active site, suggesting that differences in the loop 2 structure affect substrate recognition (Figure 2A). This loop also constitutes the region in the human LMW-PTP enzymes that arises from alternative splicing, giving rise to four isoforms [19]. In PtpA, loop 2 adopts a different orientation from that in human LMW-PTP (Figure 2A). PtpA Trp44 assumes a different conformation than the equivalent Trp49 in HPTP-B (Figure 2B), opening a groove leading to the active site. This Trp is not present in alternative isoforms of human HPTP-A or C, and has been suggested to confer substrate specificity between the human isoforms. Both Trp conformations are found in other LMW-PTP structures in this position, as well as other conformations of Trp and Tyr residues. The tyrosine residues neighboring the active site entry form a hydrophobic wall that coordinates the substrate Tyr. These Tyr residues are also shifted in PtpA compared to HPTP-B (Figure 2C). These tandem tyrosine residues

adjacent to the general acid Asp in human LMW-PTP are phosphorylated as a result of growth factor receptor activation, for example of PDGFR. Phosphorylation of Tyr131 modestly increases activity of the human enzyme, while phosphorylation of Tyr132 has no effect on enzyme activity [22]. Phosphorylated Tyr132 has instead been suggested to provide a docking site [22]. The tyrosine residues involved in human LMW-PTP regulation are structurally identical in PtpA (Tyr122 and 123), pointing to a possible regulatory role in *S.aureus* as well.

Despite the conserved fold, PTPs have highly specific substrate preferences. These differences in protein binding properties are determined by widely different surface shape and charge features [23]. Comparison of the electrostatic surface potential of PtpA and the human HPTP-B identify markedly different surface and charge topology of these enzymes. The surface of PtpA around the active site is generally less charged than that of HPTP-B, with mostly weakly negatively charged surfaces except for the strongly electropositive phosphate binding site (Figure 2C).

PtpA binds a substrate mimetic

As is commonly seen in PTP structures, a phosphate is bound in the PtpA active site. In PtpA, the negative charge of the phosphate is coordinated by five active site residues (Leu9, Gly10, Ile12, Cys13, and Arg14), forming a total of seven bonds with main chain and the Arg side chain amides. The position of this phosphate corresponds to that of substrate phosphate seen in a structure of a PTP with phosphotyrosine [24]. In addition to this substrate phosphate, clear electron density unambiguously identified a seven amino acid long peptide containing five continuous His residues (His1′-5′) followed by Gly and Ser. Thus, although proteolytically cleaved during protein purification, the His$_6$ tag co-crystallized in the PtpA active site, suggesting tight binding. Every other histidine contacts active site residues, with the intervening histidines pointing outwards into solvent (Figure 3A). The three interacting histidines form hydrogen bonds with residues Thr41, Ser88, and Asp120 that line the PtpA active site opening. Also, the following glycine residue of the peptide hydrogen bonds to the Ser95 backbone carbonyl. The imidazole ring of His1′, together with the phosphate in the active site, mimics a phosphotyrosine residue, similar to the arrangement of a phosphate and a phenylalanine binding in the active site of *M. tuberculosis* PtpB [25] (Figure 3B). Tyr122, part of the hydrophobic wall that coordinates the substrate phosphotyrosine, coordinates His1′ in a similar way to a phosphotyrosine. This arrangement suggests that the peptide is a substrate mimetic, with two other histidines also making chemically plausible interactions. His3′ and His5′ are positioned in electronegative pockets and hydrogen-bond to Ser88 and Thr44. Both histidines also engage in hydrophobic interactions via their imidazole moieties. The two histidines are complementing their binding pockets both in shape and charge: Other residues in the position occupied by His3′ and His5′ with either similarly aromatic (Trp, Tyr) or charge (Lys, Arg) characteristics would sterically clash, suggesting that binding of these histidines is reflective of true substrate binding. Based on this mode of peptide binding, we suggest a potential substrate sequence of Tyr-X-His-X-His, with X denoting any amino acid. A motif search with ProSite shows that this motif is found in only 7 *S. aureus* proteins (Figure 3C). None of these proteins is known to be phosphorylated. Because no structures of these candidate substrates are available, we used the program Phyre [26] to predict if the putative substrate sequences are accessible for phosphorylation. We obtained high confidence structural models (e-value $\leq 4 \times 10^{-18}$) that include the predicted substrate region for 6 out of the 7 proteins - only the DNA translocase FtsK model did not contain the putative substrate region. The models predict that the substrate sequences are surface-exposed, suggesting that they can serve as phosphorylation targets.

PtpA is not essential for *in vitro* growth

To begin characterizing the cellular function of the *S. aureus* LMW-PTPs, we obtained transposon mutants of both PtpA and PtpB from a random Tn5EZ library [27]. Both mutants showed similar growth rates to wild type *S. aureus* in rich (Luria Bertoni) and minimal medium (Roswell Park Memorial Institute medium), suggesting that neither PTP is essential for *in vitro* broth culture (data not shown). Because Ser/Thr phosphorylation regulates cell wall metabolism and thus permeability in *S. aureus* [28; 29], we tested the effect of LMW-PTP deletion on cell wall integrity. We did not detect any permeability phenotype of the mutants in high salt (0.625-2.5M NaCl), sodium dodecyl sulfate (1.25-5%), ampicillin (62.5-250 μg/ml), hydrogen peroxide (7.5-30%), or lysostaphin (0.025-0.1 mg/ml, with and without 2.5% sodium dodecyl sulfate) by a disc diffusion assay (data not shown), suggesting that the cell wall is largely intact in the mutant strains. The absence of a growth phenotype under these *in vitro* conditions suggests that PtpA and PtpB might mediate specialized functions during infection.

Only three tyrosine-phosphorylated proteins are currently known in *S. aureus*, the autophosphorylating tyrosine kinase CapB2, the UDP-Acetyl-Mannosamine Dehydrogenase CapO, and the heat shock chaperone HchA[9; 10]. A recent phosphoproteomics study of *B. subtilis*, a bacterium in the same phylum as *S. aureus*, identified 103 unique phosphorylation sites, among them eight on tyrosine[12]. The ratio of pSer:pThr:pTyr sites in humans is 86:12:2 compared to 70:20:10 in *B. subtilis*, suggesting that bacteria rely on pTyr signaling more heavily than eukaryotes. This finding, together with the presence of highly diverged protein tyrosine kinases in bacteria, indicates that bacteria have evolved functions and strategies of tyrosine phosphorylation distinct from those in eukaryotes.

With the rapid emergence of drug resistance in *S. aureus* and other bacterial pathogens, the identification of new classes of drug targets gains urgency. While phosphosignaling enzymes are a major class of drug targets in humans [3], their potential as antibacterials is largely undefined. Unlike bacterial tyrosine kinases, which are structurally unrelated to eukaryotic protein tyrosine kinases [30], the PtpA crystal structure underscores the striking conservation of the LMW-PTP fold between eukaryotic and bacterial enzymes. This similarity suggests that PtpA might also be a tractable drug target. However, this similarity also raises questions about the feasibility of selective inhibition of bacterial LMW-PTPs. The difficulties to design selective inhibitors that arise from the absence of large structural differences, however, is offset by the presence of only one LMW-PTP gene in humans, thus limiting the challenges of achieving selectivity. In addition, surface properties rather than differences in fold are generally mediating PTP substrate selectivity [23].

In several bacteria, the bacterial tyrosine (BY) kinases phosphorylate enzymes of the capsular biosynthesis pathway [31; 32]. The genomic location of the BY kinases and, in gram negative bacteria, the LMW-PTPs, in the cap (capsule genes) operon implicates tyrosine phosphorylation in capsule biosynthesis and transport [31; 32]. The LMW-PTPs in gram positive bacteria such as *S. aureus*, however, are encoded in operons distant from the BY kinases. Instead, members of the polymerase and histidinol phosphatases are generally encoded within the same operon as BY kinases and, in *Streptococcus* and *E. coli* dephosphorylate and directly antagonize BY kinase activation [31; 33]. Thus, PTPs in gram positive and gram negative bacteria likely control different pathways. Both *S. aureus* PTPs appear to be expressed in operons, but the flanking genes are mostly conserved hypothetical proteins that do not allow functional predictions. The absence of any permeability phenotype of the PtpA and PtpB transposon mutants suggests that PtpA and PtpB do not play a major role in cell wall synthesis. The absence of a growth phenotype in culture might point to a function during infection. Unlike the secreted virulence factor PTPs YopH from *Yersinia*

and PtpA and PtpB from *M. tuberculosis* [34], however, there is no evidence for secretion of *S. aureus* PtpA and PtpB. Yet, the PTPs could be important for metabolic shifts during infection, for example to adapt to nutrient limitation in the host.

The peptide bound in the PtpA active site offers an unexpected insight into substrate recognition. A histidine residue and the phosphate in the active site clearly mimic a substrate phosphotyrosine. The two other histidines that bind PtpA engage in plausible interactions and suggest that the true substrate(s) of PtpA also contain histidines in the equivalent positions. A search of the *S. aureus* proteome retrieved 7 sequences with a Tyr-X-His-X-His motif. These candidates provide a testable number of substrates. While none of the three previously identified phosphotyrosine proteins contain this sequence, the sequence of the putative BY kinase Cap5B1 contains a C-terminal Tyr-Tyr-His-Tyr-Tyr sequence that matches the Tyr-X-His-X-His motif except for Tyr instead of His in the last position. Interestingly, a similar Tyr-rich C-terminal sequence is the site of autophosphorylation in the second BY kinase, Cap5B2 [35]. The role of Cap5B1 is still unknown, and no tyrosine phosphorylation activity has yet been shown [36]. The substrate mimetic peptide might also prove useful as a first scaffold for inhibitor design, and the bound peptide highlights a different peptide-binding groove from HPTP-B where the groove is blocked by Trp49.

Together, our PtpA structure reveals striking similarities to human LMW-PTP as well as bacterial family members. The structure also highlights distinct differences that will aid in the design of specific inhibitors, especially in the surface charge composition of the active site and the position of the hydrophobic residues lining the active site. The peptide bound in the active site mimics a substrate peptide, offers clues to the physiologic substrates and allows for testable predictions of the substrate sequence. The cellular function of PtpA remains to be defined, but disruption of PtpA and PtpB do not affect growth in culture or cell envelope permeability, suggesting that PtpA and PtpB might have a distinct function in the context of infection.

Acknowledgments

References

1. Klevens RM, Morrison MA, Nadle J, Petit S, Gershman K, Ray S, Harrison LH, Lynfield R, Dumyati G, Townes JM, Craig AS, Zell ER, Fosheim GE, McDougal LK, Carey RB, Fridkin SK. Invasive methicillin-resistant Staphylococcus aureus infections in the United States. JAMA. 2007; 298:1763–71. [PubMed: 17940231]

2. Klein E, Smith DL, Laxminarayan R. Hospitalizations and deaths caused by methicillin-resistant Staphylococcus aureus, United States, 1999-2005. Emerg Infect Dis. 2007; 13:1840–6. [PubMed: 18258033]

3. Cohen P. Protein kinases--the major drug targets of the twenty-first century? Nat Rev Drug Discov. 2002; 1:309–15. [PubMed: 12120282]

4. Zhang ZY. Protein tyrosine phosphatases: prospects for therapeutics. Curr Opin Chem Biol. 2001; 5:416–23. [PubMed: 11470605]

5. Kannan N, Taylor SS, Zhai Y, Venter JC, Manning G. Structural and functional diversity of the microbial kinome. PLoS Biol. 2007; 5:e17. [PubMed: 17355172]

6. Shi L, Potts M, Kennelly PJ. The serine, threonine, and/or tyrosine-specific protein kinases and protein phosphatases of prokaryotic organisms: a family portrait. FEMS Microbiol Rev. 1998; 22:229–53. [PubMed: 9862122]

7. Soulat D, Vaganay E, Duclos B, Genestier AL, Etienne J, Cozzone AJ. Staphylococcus aureus contains two low-molecular-mass phosphotyrosine protein phosphatases. J Bacteriol. 2002; 184:5194–9. [PubMed: 12193638]

8. Wang WQ, Sun JP, Zhang ZY. An overview of the protein tyrosine phosphatase superfamily. Curr Top Med Chem. 2003; 3:739–48. [PubMed: 12678841]

9. Lomas-Lopez R, Paracuellos P, Riberty M, Cozzone AJ, Duclos B. Several enzymes of the central metabolism are phosphorylated in Staphylococcus aureus. FEMS Microbiol Lett. 2007; 272:35–42. [PubMed: 17498211]

10. Soulat D, Grangeasse C, Vaganay E, Cozzone AJ, Duclos B. UDP-acetyl-mannosamine dehydrogenase is an endogenous protein substrate of Staphylococcus aureus protein-tyrosine kinase activity. J Mol Microbiol Biotechnol. 2007; 13:45–54. [PubMed: 17693712]

11. Macek B, Gnad F, Soufi B, Kumar C, Olsen JV, Mijakovic I, Mann M. Phosphoproteome analysis of E. coli reveals evolutionary conservation of bacterial Ser/Thr/Tyr phosphorylation. Mol Cell Proteomics. 2008; 7:299–307. [PubMed: 17938405]

12. Macek B, Mijakovic I, Olsen JV, Gnad F, Kumar C, Jensen PR, Mann M. The serine/threonine/ tyrosine phosphoproteome of the model bacterium Bacillus subtilis. Mol Cell Proteomics. 2007; 6:697–707. [PubMed: 17218307]

13. Busso D, Delagoutte-Busso B, Moras D. Construction of a set Gateway-based destination vectors for high-throughput cloning and expression screening in Escherichia coli. Anal Biochem. 2005; 343:313–21. [PubMed: 15993367]

14. Otwinowski Z, M. W. Processing of x-ray diffraction data collected in oscillation mode. Methods in Enzymology. 1997; 276:307–326.

15. Vagin A, Teplyakov A. Molecular replacement with MOLREP. Acta Crystallogr D Biol Crystallogr. 66:22–5. [PubMed: 20057045]

16. Morris RJ, Perrakis A, Lamzin VS. ARP/wARP's model-building algorithms. I. The main chain. Acta Crystallogr D Biol Crystallogr. 2002; 58:968–75. [PubMed: 12037299]

17. Emsley P, Cowtan K. Coot: model-building tools for molecular graphics. Acta Crystallogr D Biol Crystallogr. 2004; 60:2126–32. [PubMed: 15572765]

18. Adams PD, Afonine PV, Bunkoczi G, Chen VB, Davis IW, Echols N, Headd JJ, Hung LW, Kapral GJ, Grosse-Kunstleve RW, McCoy AJ, Moriarty NW, Oeffner R, Read RJ, Richardson DC, Richardson JS, Terwilliger TC, Zwart PH. PHENIX: a comprehensive Python-based system for macromolecular structure solution. Acta Crystallogr D Biol Crystallogr. 66:213–21. [PubMed: 20124702]

19. Raugei G, Ramponi G, Chiarugi P. Low molecular weight protein tyrosine phosphatases: small, but smart. Cell Mol Life Sci. 2002; 59:941–9. [PubMed: 12169024]

20. Holm L, Rosenstrom P. Dali server: conservation mapping in 3D. Nucleic Acids Res. 38:W545–9. [PubMed: 20457744]

21. Zhang M, Stauffacher CV, Lin D, Van Etten RL. Crystal structure of a human low molecular weight phosphotyrosyl phosphatase. Implications for substrate specificity. J Biol Chem. 1998; 273:21714–20. [PubMed: 9705307]

22. Bucciantini M, Chiarugi P, Cirri P, Taddei L, Stefani M, Raugei G, Nordlund P, Ramponi G. The low Mr phosphotyrosine protein phosphatase behaves differently when phosphorylated at Tyr131 or Tyr132 by Src kinase. FEBS Lett. 1999; 456:73–8. [PubMed: 10452533]

23. Barr AJ, Ugochukwu E, Lee WH, King ON, Filippakopoulos P, Alfano I, Savitsky P, Burgess- Brown NA, Muller S, Knapp S. Large-scale structural analysis of the classical human protein tyrosine phosphatome. Cell. 2009; 136:352–63. [PubMed: 19167335]

24. Salmeen A, Andersen JN, Myers MP, Tonks NK, Barford D. Molecular basis for the dephosphorylation of the activation segment of the insulin receptor by protein tyrosine phosphatase 1B. Mol Cell. 2000; 6:1401–12. [PubMed: 11163213]

25. Grundner C, Ng HL, Alber T. Mycobacterium tuberculosis protein tyrosine phosphatase PtpB structure reveals a diverged fold and a buried active site. Structure. 2005; 13:1625–34. [PubMed: 16271885]

26. Kelley LA, Sternberg MJ. Protein structure prediction on the Web: a case study using the Phyre server. Nat Protoc. 2009; 4:363–71. [PubMed: 19247286]

27. Burnside K, Lembo A, de Los Reyes M, Iliuk A, Binhtran NT, Connelly JE, Lin WJ, Schmidt BZ, Richardson AR, Fang FC, Tao WA, Rajagopal L. Regulation of hemolysin expression and virulence of Staphylococcus aureus by a serine/threonine kinase and phosphatase. PLoS One. 5:e11071. [PubMed: 20552019]

28. Beltramini AM, Mukhopadhyay CD, Pancholi V. Modulation of cell wall structure and antimicrobial susceptibility by a Staphylococcus aureus eukaryote-like serine/threonine kinase and phosphatase. Infect Immun. 2009; 77:1406–16. [PubMed: 19188361]

29. Tamber S, Schwartzman J, Cheung AL. Role of PknB kinase in antibiotic resistance and virulence in community-acquired methicillin-resistant Staphylococcus aureus strain USA300. Infect Immun. 78:3637–46. [PubMed: 20547748]

30. Grangeasse C, Terreux R, Nessler S. Bacterial tyrosine-kinases: structure-function analysis and therapeutic potential. Biochim Biophys Acta. 1804:628–34. [PubMed: 19716442]

31. Grangeasse C, Cozzone AJ, Deutscher J, Mijakovic I. Tyrosine phosphorylation: an emerging regulatory device of bacterial physiology. Trends Biochem Sci. 2007; 32:86–94. [PubMed: 17208443]

32. Vincent C, Duclos B, Grangeasse C, Vaganay E, Riberty M, Cozzone AJ, Doublet P. Relationship between exopolysaccharide production and protein-tyrosine phosphorylation in gram-negative bacteria. J Mol Biol. 2000; 304:311–21. [PubMed: 11090276]

33. Morona JK, Morona R, Miller DC, Paton JC. Streptococcus pneumoniae capsule biosynthesis protein CpsB is a novel manganese-dependent phosphotyrosine-protein phosphatase. J Bacteriol. 2002; 184:577–83. [PubMed: 11751838]

34. Cozzone AJ. Role of protein phosphorylation on serine/threonine and tyrosine in the virulence of bacterial pathogens. J Mol Microbiol Biotechnol. 2005; 9:198–213. [PubMed: 16415593]

35. Olivares-Illana V, Meyer P, Bechet E, Gueguen-Chaignon V, Soulat D, Lazereg-Riquier S, Mijakovic I, Deutscher J, Cozzone AJ, Laprevote O, Morera S, Grangeasse C, Nessler S. Structural basis for the regulation mechanism of the tyrosine kinase CapB from Staphylococcus aureus. PLoS Biol. 2008; 6:e143. [PubMed: 18547145]

36. Soulat D, Jault JM, Duclos B, Geourjon C, Cozzone AJ, Grangeasse C. Staphylococcus aureus operates protein-tyrosine phosphorylation through a specific mechanism. J Biol Chem. 2006; 281:14048–56. [PubMed: 16565080]
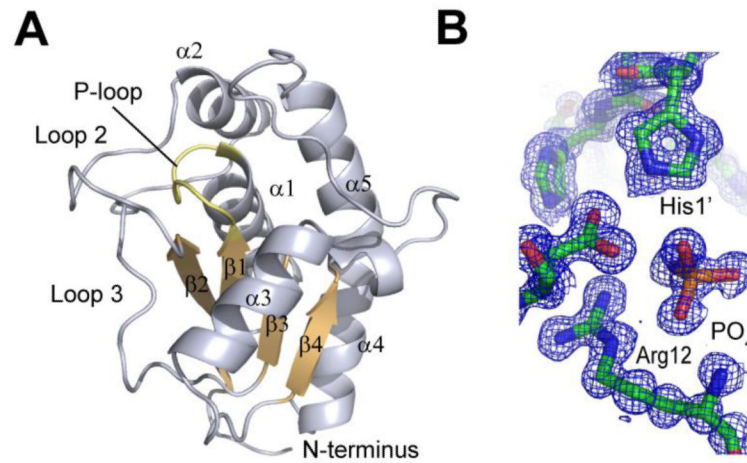
Figure 1.
Overall structure of PtpA. **A.** Cartoon representation of PtpA showing the central four-stranded β-sheet (orange) and the active-site P-loop (yellow). **B.** $2F_o$-F_c electron density map of the active site region contoured at 1σ shows phosphate, Arg12, and a histidine residue from the bound peptide. All images were generated in PyMol.
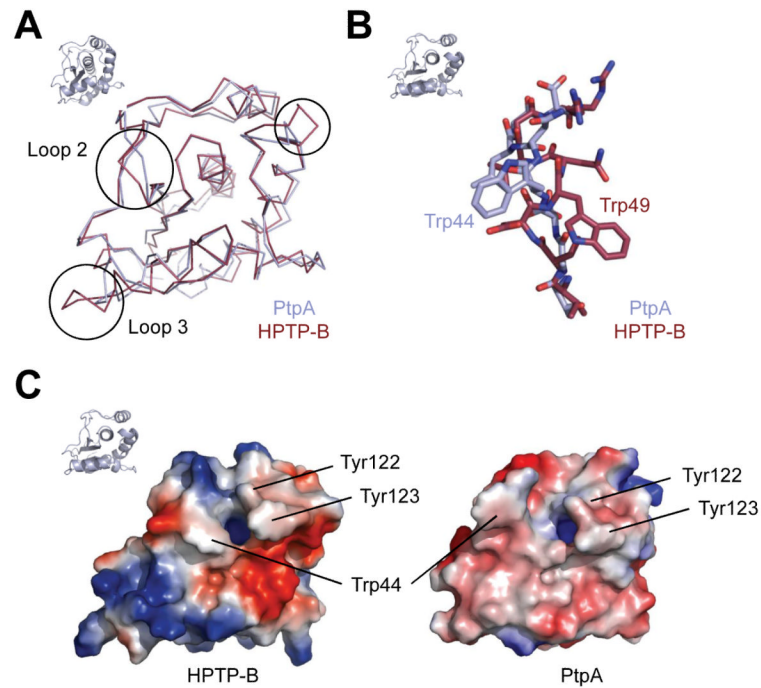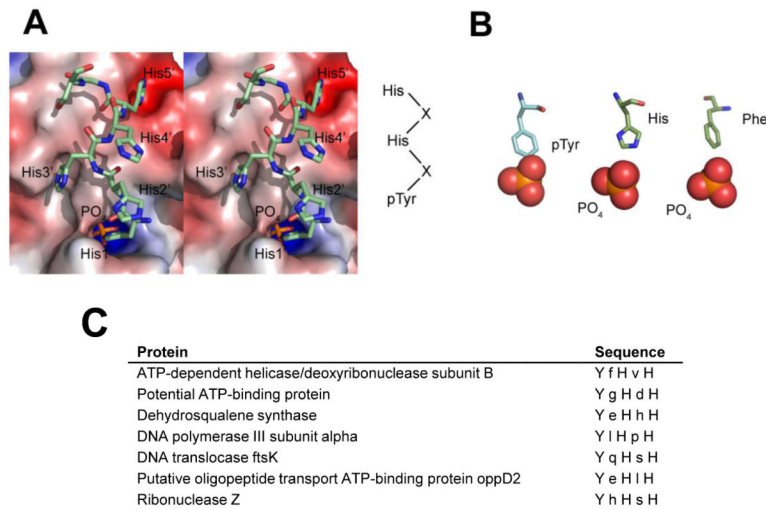
Figure 2.
Similarities and differences to human LMW-PTP. **A.** An overlay of human HPTP-B and PtpA in ribbon representation shows close similarity of the overall folds. Major differences (circles) are visible in some regions, including loop 2, which contributes to shaping the peptide binding site. **B.** Loop 2 of PtpA adopts a different orientation from that of HPTP-B, positioning Trp44 in the opposite direction from the equivalent Trp49 in HPTP-B. This shift allows for peptide binding in PtpA. **C.** Electrostatic surface potential shows clear charge differences in the direct vicinity of the active site entry (blue opening), and the shift of the hydrophobic wall and Trp44 compared to HPTP-B. Orientation of PtpA is indicated by small cartoon representation in top left corner.

Figure 3.
Peptide binding to PtpA. **A.** Stereo view of the peptide bound in the active site in sticks representation. The peptide binds with every other histidine to charge-complementary PtpA surfaces, suggesting a substrate sequence of pTyr-X-His-X-His. **B.** Phosphotyrosine and phosphotyrosine mimetics bound in PTP active sites. In PtpA, one histidine and a phosphate mimic a phosphotyrosine substrate, similar to the arrangement of Phe222 and phosphate in the structure of *M. tuberculosis* PtpB (PDB-ID 1YWF). A substrate phosphotyrosine peptide bound to PTP1B (PDB-ID 1G1F) is shown on the left for comparison. **C.** The seven *S. aureus* proteins that contain the potential substrate motif Tyr-X-His-X-His.

Table 1

Crystallographic data and refinement statistics for PtpA. Parenthesis denote values for the highest-resolution shell.

Data Collection and Refinement Statistics	
Data Collection	
Space group	P12$_1$1
Unit cell dimensions	
a, b, c (Å)	34.81, 35.1, 65.51
β, β, γ (°)	90, 91, 90
Resolution (Å)	35.1-1.03
Wavelength (Å)	1.11587
R$_{merge}$ (%)	4.3 (47)
Completeness (%)	93.7 (88.8)
Multiplicity	2.4 (2.4)
I/σI	13.8 (2.2)
Refinement statistics	
Resolution (Å)	34.8-1.03
Reflections	69482
R$_{work}$/R$_{free}$ (%)	15/16.8
Number of atoms	
Protein atoms	2654
Waters	297
Rms Δ bonds (Å)	0.013
Rms Δ angles (°)	1.42
Average B-factor (Å^2)	13.9
Main chain dihedral angles	
Most favored (%)	98.2
Allowed (%)	1.8
Disallowed (%)	0